MODELING SEDIMENT DEPOSITION FOR PREDICTING MARSH HABITAT DEVELOPMENT

Michelle Newcomer, San Francisco State University
Amber Kuss, San Francisco State University
Tyler Ketron, Stanford University
Alex Remar, Cal Poly San Luis Obispo
Vivek Choksi, Gunn High School
Karen Grove, Ph.D., San Francisco State University
J. W. Skiles, Ph.D., NASA Ames Research Center
DEVELOP NASA Ames Research Center
M.S. 242-4 Moffett Field, California 94035
Michelle.E.Newcomer@nasa.gov
Joseph.W.Skiles@nasa.gov

ABSTRACT

The South Bay Salt Pond Restoration Project (SBSPRP) is the largest tidal wetland restoration project on the west coast of the United States. The purpose of this project was to use *in-situ* and remote sensing measurements to create a GIS model capable of predicting sediment deposition in restored ponds in the Alviso Salt Pond Complex. A sediment transport model, suspended sediment concentration maps, as well as laboratory analyses of *in-situ* sediment data were used to predict sediment deposition. Suspended sediment concentrations from our *in-situ* samples as well as the USGS's continuous monitoring sites were correlated with Landsat TM 5, ASTER, and MODIS reflectance values using three statistical techniques—an Artificial Neural Network (ANN), a linear regression, and a multivariate regression to map suspended sediment concentrations in the South Bay. Multivariate and ANN regressions using ASTER proved to be the most accurate correlation method, yielding R^2 values of 0.88 and 0.87 respectively. Sediment grain size data were collected from Pond A21 to determine particle settling velocities, grain size distribution, bulk densities, and rates of deposition. These data coupled with tidal frequencies and suspended sediment maps were used in the Marsh Sedimentation (MARSED) model for predicting deposition rates for three years. Data from MODIS were used to track sediment transport pathways in the South Bay for further assessing future marsh development. Results from this project were applied to the Regional Ocean Modeling System (ROMS) sediment transport module for understanding sediment dynamics in the South Bay. MARSED results for Pond A21 show an RMSD of 66.8mm ($< 1\sigma$) between modeled and field observations and can therefore be successfully used to model future wetland restoration efforts.

KEYWORDS: sediment modeling, GIS tool, Landsat TM, ASTER, suspended sediment concentration (SSC)

INTRODUCTION

Development of the San Francisco Bay Estuary during the last 200 years has transformed nearly 90% of historical wetland habitats into agricultural fields and industrial salt production ponds (Philip Williams & Associates Ltd. and Faber, 2004). Tidal influences in these areas were halted through a system of dikes, subsequently altering the sediment budget and vegetation distribution and contributing to an overall loss of biodiversity (Philip Williams & Associates Ltd. and Faber, 2004). The South Bay Salt Pond Restoration Project (SBSPRP), the largest and most complex wetland restoration effort on the west coast of the United States, will convert approximately 15,000 acres of salt production ponds to restored wetland habitats (Takekawa et al., 2005). The SBSPRP is managed collaboratively by the California State Coastal Conservancy (CSCC), the U.S. Fish and Wildlife Service (FWS), and the California Department of Fish and Game (DFG) (Trulio et al., 2007). Understanding long-term sediment dynamics within the South Bay is critical for proper accumulation estimates and subsequent restoration management strategies in newly breached salt ponds (Foxgrover et al., 2007). Accumulation rates of breached salt ponds are directly influenced by suspended sediment concentrations (SSC), water flow paths, and tidally-driven sediment re-suspension (Philip Williams & Associates Ltd. and Faber, 2004). Marshland rise within the breached salt ponds

allows for plant colonization, and establishment of a healthy wetland ecosystem (Philip Williams & Associates Ltd., 2005). Continued monitoring of estuarine sediment accumulation will provide temporal and spatial development predictions for each phase of the restoration process.

The purpose of this project is to use remote sensing technology to model and analyze sediment deposition within Island Pond A21 for the three years after its levees were breached in March, 2006 (Figure 1). Sediment deposition can be estimated from SSC, settling velocity, bulk density, and water velocity (Temmerman et al., 2004). Temmerman et al. (2003) modified an algorithm developed by Krone (1987) to predict sediment deposition using these known variables, and was able to predict sediment deposition in growing marsh ecosystems at point locations of known SSC. This project used point locations of SSC to calibrate remote sensing imagery, providing a spatially comprehensive distribution of SSC within Pond A21. Accurately mapping suspended sediment concentrations from remotely sensed images provided a method for determining sediment concentrations without disturbing ecologically sensitive areas. Additional inputs of seasonal variations in SSC, distance from the levee breech, bulk density, settling velocity, marsh height, time of inundation, and a high-volume array of SSC data points (obtained from the satellite-produced images) were then used in the Marsh Sedimentation (MARSED) model for sediment accumulation (Temmerman et al., 2004). Modeled results were compared with field measurements of sediment accumulation obtained by Callaway et al. (2009). Areas of interest to the SBSPRP addressed in this project include understanding sources and sinks for sediment, obtaining sediment accumulation locations, establishing a timeline of marsh development for yet-to-be breached Pond A6, and providing managers with a more reliable GIS mapping tool for sediment accumulation estimates. This GIS model can be applied to a variety of environments and will aid in future restoration efforts.

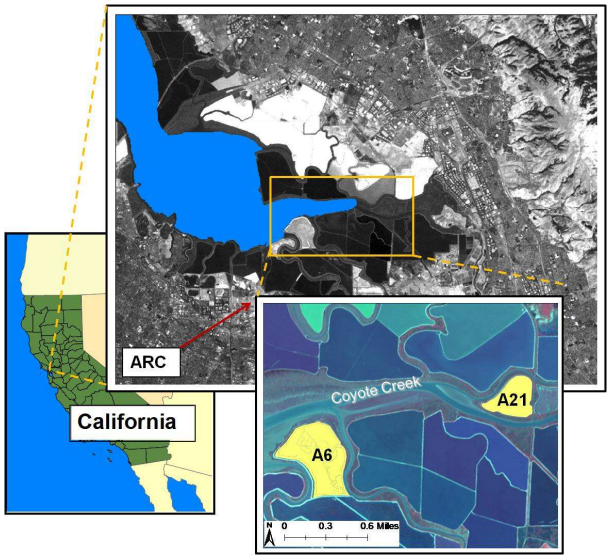

Figure 1. Study location in the Alviso Complex in the San Francisco Bay, California. Ponds A21 and A6 are shown in yellow. Note also the location of Coyote Creek.

METHODOLOGY

Remote sensing has previously been used to calibrate reflectance values of SSCs in the visible and near-infrared spectral range to in-situ measurements, thus creating a large spatial data range (Munday and Alföldi, 1979; Chen et al., 1992; Baban, 1995; Miller and McKee, 2004; Chen et al., 2006). Three different satellite sensors—the Landsat-5 Thematic Mapper, the Advanced Spaceborne Thermal Emission and Reflection Radiometer (ASTER), and the Moderate Resolution Imaging Spectroradiometer (MODIS)—were used in this project to map suspended sediment in the South San Francisco Bay. Reflectance values were statistically correlated with suspended sediment concentrations from *in-situ* field data collected during the summer of 2010 and from the USGS Water Quality Dataset. Linear regression, multivariate regression, and Artificial Neural Networks (ANNs) were used to correlate pixel reflectance values with corresponding SSC measurements. The finalized SSC maps were then input into the MARSED model in order to model deposition in Pond A21 for three years post-breach. GIS values of modeled marsh accumulation were then compared to previously documented point measurements of sediment accumulation heights in the breached Island Pond A21 (Callaway et al., 2009) to assess model accuracy. Finally, sediment transport was modeled and visualized in the South Bay using the ROMS model and input datasets from our laboratory analysis and GIS/remote sensing results.

Field Methods

Various studies have developed methods for monitoring sediment accumulation rates, with a wide-range of techniques and accuracy. Installed monitoring devices such as: sediment traps (Gardner et al., 1980; Bale, 1998), graduated pins (Reed, 1989; Cahoon and Lynch, 1997; Callaway et al., 2009), anchored tiles (Reed, 1989; Pasternack and Brush, 1998), and sediment erosion tables (SETs) (Boumans and Day, 1993; Childers et al., 1993;

Cahoon et al., 2002) are inexpensive and effective methods for estimating accumulation rates, but provide limited sampling points. SSC estimates are often used to indirectly measure sediment accumulation rates, and can be obtained through *in-situ* measurements and remote sensing techniques (Stumpf and Pennock, 1989; Froidefond et al., 1993; Ruhl et al., 2001; Li et al., 2003; Miller and McKee, 2004). Surface water samples for suspended sediment analysis were collected at 24 locations in the South Bay over the course of two field days that corresponded with Landsat and ASTER overpasses. Samples were processed at the USGS Western Coastal and Marine Geology Laboratory (WCMGL) for suspended sediment concentrations. In addition, sediment samples were collected from Pond A21 to characterize the physical properties of sediment in the South Bay. These samples were taken at five representative locations along the perimeter and seven locations on the interior of the pond. Each sample was processed at the USGS WCMGL for grain size distribution, settling velocity, and organic content. These characteristics, along with suspended sediment concentrations, are inputs for the MARSED model (Temmerman et al., 2003; Temmerman et al., 2004).

USGS Laboratory Analysis

Samples were processed at the USGS WCMGL in Menlo Park, California. Water samples were analyzed for suspended sediment concentration, and sediment samples were analyzed for grain size distribution, settling velocity, and organic carbon content (Table 1). A value for bulk density was generated from a reference density data set of clay and mud densities (SI Metric, 2009). The resulting data were input into the MARSED model.

Table 1. Variables and laboratory processing procedure

Variable	Field Collection Method	Laboratory Processing Technique
Suspended sediment concentration (mg/L)	Water samples from South Bay	Filtration
Grain size distribution	Sediment samples from Pond A21	Coulter LS100Q using laser diffraction
Settling velocity (cm/s)	Sediment samples from Pond A21	Modified Gibbs equation
Organic carbon content (% organic carbon)	Sediment samples from Pond A21	CO_2 coulometer and combustion chamber

USGS Continuous Monitoring Stations and Monthly Cruises

Calculated suspended sediment concentrations from January, 2000 to May, 2010 were obtained from the USGS's Water Quality of San Francisco Bay database for sampling stations 30 to 36, south of the San Mateo Bridge (USGS, 2007). Outliers due to sensor interference from biological fouling, especially during summer months, were excluded (Buchanan and Lionberger, 2007). Seasonal mean averages were computed and compared to the 10-year average of 35.20 mg/L. The ratio between seasonal average suspended sediment concentrations and the 10-year average was calculated to be 1.08 for winter, 1.16 for spring, 0.95 for summer, and 0.81 for fall. This seasonal variation in suspended sediment concentrations can be explained by high rainfall in the winter and spring. Re-suspension of sediments may have also contributed to higher concentrations in the spring and summer months, when the South Bay's strong winds drive re-suspension (Buchanan and Lionberger, 2007). These seasonal coefficients were applied to seasonally adjust predicted suspended sediment concentrations for input into the MARSED model. Historical suspended sediment concentrations from the USGS's Water Quality of San Francisco Bay and Continuous Monitoring in the San Francisco Bay and Delta datasets were used for further analysis and calibration of the satellite imagery.

Satellite Remote Sensing

All satellite imagery was geometrically and radiometrically corrected to reflectance and re-projected to the UTM WGS 84 North projection to ensure tonal and spatial comparability between each scene using Earth Resources Data Analysis System (ERDAS) Imagine software. To create SSC maps, images were imported into a Geographical Information System (ArcGIS), and pixel reflectance values were extracted and correlated with SSC values at point locations. Using known UTM coordinates, the location of each *in-situ* measurement was identified on the corrected satellite images. A 3x3 pixel grid closest to each *in-situ* location was selected and reflectance values were averaged. These representative values were calibrated with known SSCs using the statistical techniques outlined below to map the distribution of suspended sediment throughout the South Bay. These maps were used in the MARSED GIS model for the SSC variable.

Landsat TM5 and ASTER. Imagery from the Landsat TM 5 and ASTER were used to create predictive maps of SSCs at the water surface. Imagery was calibrated using data from the USGS Water Quality of San Francisco Bay monitoring program (USGS, 2010a; USGS, 2010b) and from our own sampling campaign. Values were determined at both the original resolution and at an averaged resolution to reduce signal noise. Linear, multivariate, and ANN regressions were compiled for both sensors to determine the best statistical technique for correlation with SSC. Using these relationships a SSC map was created. Sensors and bands used, resolution, and purpose are described in Table 2.

MODIS. MODIS images were downloaded and applied with a standard data correction coefficient. There were two objectives for using MODIS imagery: to calibrate with SSC values, and to map sediment transport in a plume after a storm event. Band 2 (841-876 nm) represented the most statistically significant correlation to SSC reflectance, and was therefore used to track flow direction of a sediment plume during cloud-free days. Precipitation data were obtained from the National Oceanic and Atmospheric Administration's (NOAA) National Climate Data Center (NCDC), and storm events were selected based on daily precipitation totals from 35 stations located in the 20 northern California counties near the San Francisco Bay. Two moderate storm events were identified with associated cloud-free MODIS images, occurring on January 1st, 2006 and January 1st, 2009, respectively. The 2006 sequence included MODIS images from two, four, and seven days following the storm event, and the 2009 sequence included MODIS images from eight, nine, and ten days following the storm event (Figure 2). MODIS images were also calibrated using data from the USGS Water Quality of San Francisco Bay monitoring program (USGS, 2010b).

Table 2. Satellite sensors used, bands, resolution, dates, and source of data.

Sensor	Purpose	Bands Used	Wavelengths (µm)	Resolution (m)	Dates used	Image Source
MODIS on Terra	Detect relative SSCs to track sediment transport	1 2	0.62-0.67 0.84-0.87	250	1/4/06, 1/6/06, 1/9/06, 1/9/09, 1/10/09, 1/11/09	WIST
ASTER on Terra	Detect SSCs	3	0.52-0.86	15	10/8/04, 10/29/09	Glovis (USGS, 2010a)
Landsat 5 TM	Detect SSCs	3	0.45-0.69	30	8/18/94, 8/22/07, 8/27/09, 7/5/10	Glovis
Hyperion on EO-1	Detect relative SSCs	20 52 104	0.548 0.874 1.184	30	3/26/10, 7/7/10	Glovis

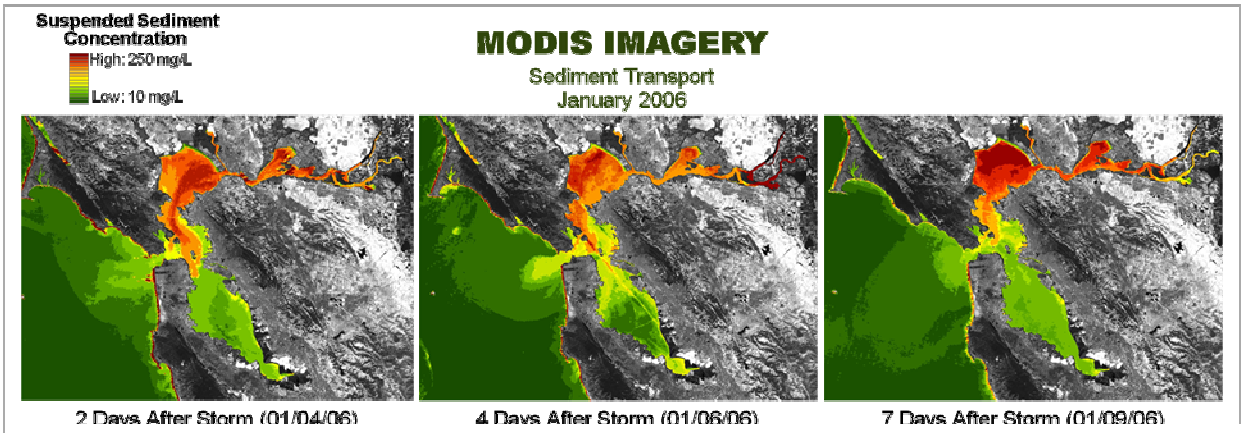

Figure 2. MODIS sediment transport time series. High sediment concentrations begin 2 days after the storm with the highest concentrations seen one week after.

Statistical Techniques

Three different statistical techniques were used to establish correlations between SSCs and reflectance values (Teodoro et al., 2008): linear regression, multivariate regression, and an ANN. For linear regressions, the band that produced the best statistical correlation for each sensor was determined and then used in subsequent calculations. For multivariate regressions and artificial neural networks, all available visible and near-infrared bands were used. The ANN was implemented using an adaptive linear combiner (Wilde, 2009). The ANN estimates the SSC by multiplying each band by a weight. After each iteration the residual is calculated, and the weights are adjusted until the error is minimized (Figure 3). Essentially, the ANN takes the data and learns from it until it produces the lowest possible error. Field SSC measurements as well as data from the USGS's Water Quality of the San Francisco Bay Project were correlated with reflectance values from multiple satellite images using all of these statistical techniques (USGS, 2010b). The final maps were then used in the MARSED model for predicting sediment deposition.

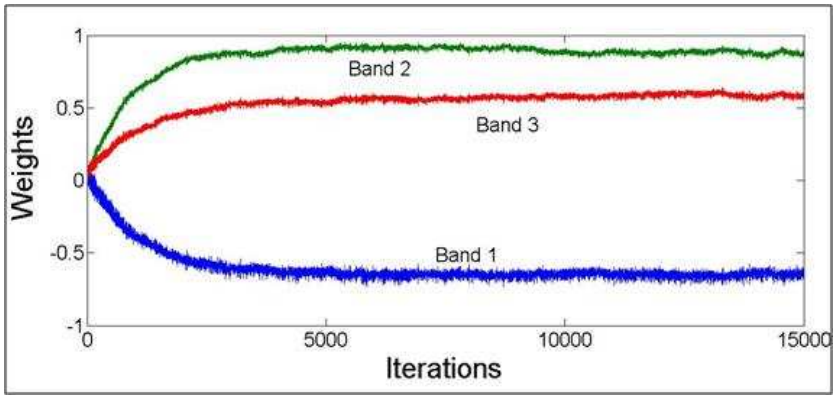

Figure 3. ANN linear combiner weights

Sediment Deposition Model

A goal of this project was to model sediment deposition in Pond A21 and compare modeled results with results obtained by Callaway et al. (2009). Modeling techniques can be used to estimate future sediment accumulation rates, and account for factors including wetland age, surface elevation, and sea level fluctuations (Allen, 1990; French and Spencer, 1993; French et al., 1995; Allen, 1997; Temmerman et al., 2003; Temmerman et al., 2004). A zero-dimensional time-stepping marsh sediment accumulation model (MARSED) has been used to predict wetland development based on particle settling velocity, time dependant SSC, and sediment bulk density (Temmerman et al., 2003; Temmerman et al., 2004). To effectively model sediment accumulation over several tidal cycles and years, the MARSED model developed by Krone (1987), and modified by Temmerman et al., (2004),was implemented in GIS to predict sediment accumulation for Pond A21, and then an accuracy assessment was run to verify simulated results from Equation 1.

Equation (1)

$$\frac{dE}{dt} = \frac{dS(grain)}{dt} + \frac{dS(organic)}{dt} - \frac{dP}{dt}$$

Where:
dE/dt = final marsh height rise (m/year)
dS(grain)/dt = rate of mineral sediment deposition (m/year)
dS(organic)/dt = rate of organic content deposition (m/year)
dP/dt = resuspension/compaction (m/year)

Equation 1 was solved for *dE/dt* by summing the rates of deposition for mineral sediment and organic content and subtracting re-suspension and compaction. Organic content was obtained from the laboratory analysis and solving for the addition of sediment grains, *dS(grain)/dt*, required further calculation in Equation 2. Equation 2 provides the total grain deposition by calculating deposition for each tidal cycle and subsequently for each year. Equation 2 produced a final estimate of marsh evolution during the three years post-breach as a function of the concentration, the settling velocity, and the bulk density of the sediment grains (Krone, 1987).

Equation (2)

$$\frac{dS(grain)}{dt} = \int_{Year}\int_{Tide} \frac{w_s * C(t)dt}{\rho}$$

Where:
dS(grain)/dt = rate of mineral sediment deposition (m/year)
w_s = particle settling velocity (m/s)
C(t) = time dependant concentration from Equation 3 (kg/m^3), obtained here using remote sensing
ρ = bulk density (kg/m^3)

To obtain the *C(t)* term in Equation 2, the initial concentration value *C(0)* was taken from the remote sensing image, and then the ordinary differential equation (Equation 3) was solved for *dC/dt* for initial conditions at *t = 0.* Euler's Method was used for solving the equation by iteration through each time step to obtain the final *C(t)* at each time step until the solution reached a steady-state value (Figure 3). To initially model the changing concentration with the incoming tide, Equation 3 was solved at time steps of 0.001s in Matlab (Krone, 1987; Temmerman et al., 2003).

Equation (3)
$$[h(t)-E]\frac{dC}{dt} = -w_s C(t) + [C(0)-C(t)]\frac{dh}{dt}$$

Where:
h(t) = time dependant water surface elevation (m)
E = Elevation of the marsh surface (m)
dC/dt = rate of concentration change (kg/s)
w_s = particle settling velocity (m/s)
C(t) = time dependant concentration (kg/m^3)
C(0) = initial concentration (kg/m^3)
dh/dt = velocity of incoming flood tide (m/s)

For the purposes of this study, the Euler method yielded sufficiently accurate results. The numerical approximation for solving Equation 3 at time steps of 0.001s and 60,000+ iterations ensured a steady-state solution was reached (Figure 3). Euler's method was appropriate for solving Equation 3 because the Euler global error is proportional to the time step—approximately ± 0.001mg/l in this case. This error is insignificant to the overall SSC concentration values because the accuracy of the SSC concentration is ±0.01 mg/l. Because the magnitude of error for Euler's method was much lower than the accuracy of our SSC concentrations, this method provided a reasonable approximation to the final suspended sediment concentration values.

A conceptual model of the MARSED model is shown in Figure 4. All of the inputs are considered in this study as directly affecting marsh sedimentation and were applied to the GIS model. Variables such as distance from breach, and initial marsh height directly affect marsh sedimentation because sedimentation will change based on these variables. Suspended sediment concentration, *C(t)*, was the most influential variable in this study and was provided by the remote sensing images. For each pixel, *C(0)* was provided by the image and was allowed to run through Equation 3 to determine the final rate of concentration change *dC/dt*. Once the rate of concentration change was obtained, the concentration at any specific time thereafter could be solved.

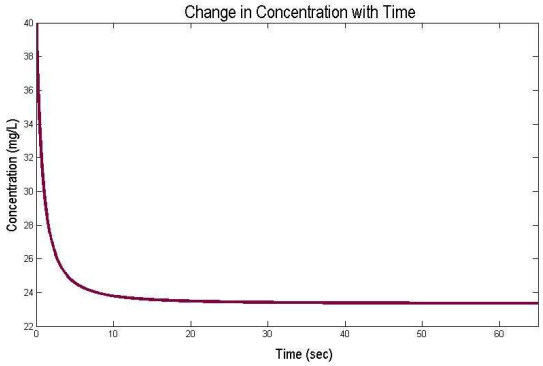

Figure 3. The change in concentration with each time step.

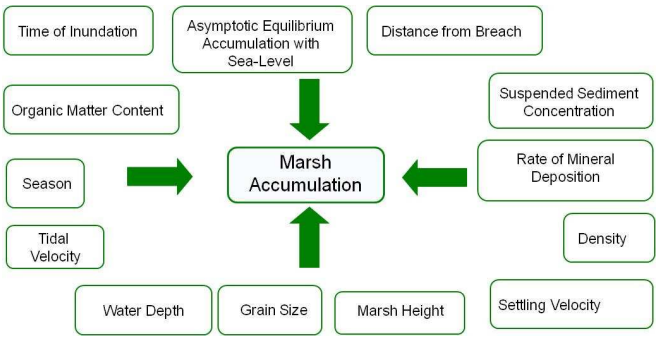

Figure 4. Conceptual model of Marsh Accumulation.

ROMS Hydrodynamic Model

Final sediment deposition locations and transport have been modeled using multiple applications, most notably the Regional Ocean Modeling System (ROMS) which simulates non-linear flow dynamics (Haidvogel et al., 2008). To better understand the forces affecting sediment dynamics in the study area, an ocean circulation model was programmed for the San Francisco Bay. ROMS was chosen as an appropriate model due to its high accuracy and adaptability (Haidvogel et al., 2008). Although the model output was course due to the small scale of the study area, the simulation was useful in identifying possible sources of sediments and to explain trends in SSC. For example, the calibrated sediment maps consistently showed a region of higher than average SSC in the North San Francisco Bay. After the ROMS simulation was allowed to equilibrate, an eddy formed in this region of the Bay. This circulation pattern, along with the high influx of sediments from the Sacramento-San Joaquin River Delta, causes sediment to accumulate possibly accounting for the high SSC in the North Bay. Future study would involve expansion and refinement of the model and the inclusion of a sediment transport module.

RESULTS AND DISCUSSION

Field and Laboratory Results

All of the field samples were processed at the USGS WCMGL. The average values from this analysis that were used in the MARSED model are shown in Table 3. Average surface suspended sediment concentrations for pond A21 were 46.16 mg/L. This is consistent with the values provided by the multivariate regression for Pond A21 using the RS images. This field validation of the multivariate correlation is another source of information that provides the best possible SSC map for input into the MARSED model.

Table 3. Average values of field, laboratory, and reference data.

Variable	Average Value
Surface suspended sediment concentration (mg/L)	46.16
Grain size (µm)	4.72
Settling velocity (m/s)	5.06×10^{-5}
Organic carbon content (% organic carbon)	2.08
Bulk density (kg/m^3)	1600

The low organic content of sediment in our samples can be attributed to the fact that Pond A21 is a continuously developing marsh with little biological activity. The sediment is dominated by clay sized particles—92% of particle diameters fall below 16 µm.

Statistical Techniques for Predicting Suspended Sediment

The accuracy of detecting SSCs through the use of remote sensing is dependent on many factors including the resolution of the satellite image, the ability to acquire and process the image, and hydrodynamic influences. The three remote sensing instruments used in this study (ASTER, Landsat TM 5, and MODIS) show varying accuracy in correlating reflectance values with SSCs (Table 4). Reflectance values in clear water are generally zero, and predictably increase with rising suspended sediment concentrations (Li et al., 2003). Regressions effectively correlated pixel values with SSCs in each of the sensors, and were subsequently applied to each image in ArcGIS to create a suspended sediment map. The most effective band for SSC correlations from ASTER and Landsat TM 5 was band 3, while band 2 provided the most accurate correlation for MODIS. These bands all occur in the near-infrared range, which has been proven to be

Table 4. R^2 values by sensor and statistical technique.

Sensor	Linear	Multivariate	ANN
Landsat 5 TM	0.57 (Band 3)	0.84	0.69
ASTER	0.65 (Band 3)	0.88	0.87
MODIS	0.84 (Band 2)	0.84	0.84

the most effective spectral range for mapping suspended sediment (Li et al., 2003). Multivariate and ANN regressions using ASTER imagery proved to be the most accurate correlation method, yielding R^2 values of 0.88 and 0.87 respectively. A proportional relationship between image resolution and SSC mapping accuracy was evident. The 15 m resolution of ASTER produced the most accurate results in correlating SSC concentrations.

MODIS imagery was used to effectively monitor plume movement within the entire San Francisco Bay system. Tracking the movement of plumes following major storm events aids in detecting the source of sediment and the time it takes for sediment arrival. Due to the coarse resolution of MODIS (250 m) and the frequency of image acquisition (daily), it is best suited for tracking sediment movement rather than mapping SSCs. MODIS linear regressions show a R^2 value of 0.68 for band 1 and a R^2 value of 0.84 for band 2. MODIS multivariate regression show a R^2 value of 0.84 for bands 1 and 2 combined. MODIS ANN regressions show a R^2 value of 0.84 for bands 1 and 2 combined. MODIS transport maps created from these regressions also demonstrates that sediment not only originates from the Sacramento-San Joaquin Delta, but also from Coyote Creek.

GIS Model Results

The MARSED model can accurately predict marsh sedimentation in the newly breached salt ponds in the South San Francisco Bay. The accuracy of the MARSED model is dependent on field data and GIS inputs. Root mean square deviation (RMSD) was used to measure the difference between marsh accumulation values computed by the model and those measured by Callaway et al. (2009) (Figure 5a). Linear regression with band 3 of ASTER provided the most accurate results, yielding a RMSD of 66.84 mm (Table 5). This is less than 3 inches of deviation indicating that this is an acceptable model for predicting marsh sedimentation. In this case, the linear technique produced the lowest RMSD for the model, whereas multivariate regression produced the best correlation between SSC and reflectance (Table 4). Furthermore, linear regression, being the simplest statistical method used, was not expected to produce the most accurate marsh accumulation estimates. This discrepancy could have resulted from bias in the model, which systematically overestimated marsh accumulation. This overestimation most likely arose because the model does not account for compaction or re-suspension of settled sediment—processes which inhibit marsh elevation rise. Re-suspension may be wind-generated (driven by shear velocity and water depth) or tidally generated (when ebb tide moves water and sediment out of the ponds). The inherent error of the model can also be attributed to the deviation of the reflectance values from the true SSC values. Reflectance values are measured to the fifth decimal place, whereas SSC concentrations are reported as whole values. This discrepancy could result in multiple reflectance values for the same SSC value, increasing error in the analysis. The cumulative marsh sedimentation curve is shown in Figure 5b. The marsh initially rises rapidly, but sedimentation rates slow as the marsh nears a stable elevation that allows for vegetation colonization.

Table 5. Accuracy assessment of the GIS modeled results.

	RMSD
ASTER Linear	66.84
ASTER ANN	82.32
ASTER Multivariate	97.94
Landsat Linear	120.41
Landsat ANN	131.83
Landsat Multivariate	186.84
MODIS Linear	274.11
MODIS ANN	275.41
MODIS Multivariate	281.24

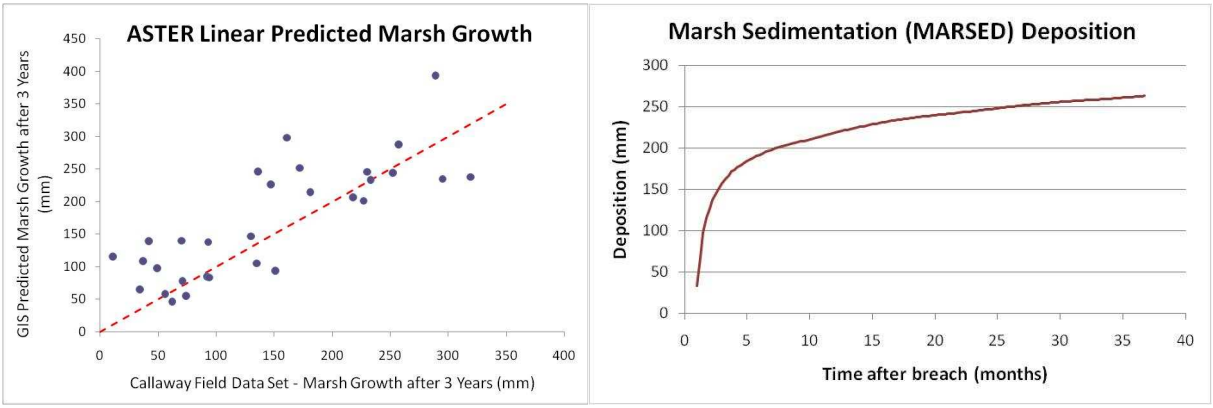

Figure 5. a) GIS predicted sediment deposition vs. field data set, b) Marsh height modeled over time.

Although the model produced acceptable results, outliers indicate a need for further assessment of environmental variables. Four outliers greatly underestimated sediment accumulation in the model, and were not included in the RMSD calculations. These outliers corresponded with locations along the southeastern perimeter of Pond A21, where unaccounted influences from the tidal channel and from pond geometry may have significantly heightened true marsh accumulation. When outliers were excluded, the model's RMSD of 66.84 mm fell within one standard deviation of actual accumulation values. Because of this high accuracy, the model is a useful tool for studying future wetland restoration efforts.

Pond A6 Model Run

The MARSED model was applied to Pond A6 in the Alviso complex, which is scheduled for levee breaching in the Fall of 2010. An initial run-through of the model with the same rates of deposition and initial conditions as for Pond A21 did not yield marsh equilibrium levels to provide a stable habitat for vegetation colonization within a 36-month time frame. The model was then run for a longer time frame, yielding equilibrium levels after 60 months. One interpretation is that a longer time frame was necessary because SSCs are consistently lower (by about half) around A6 than around A21, leaving less sediment for deposition and resulting in lower marsh accumulation rates in A6. The location of the levee breaches also factored into the longer time frame for marsh establishment in A6 (Figure 6). Pond A6 has two proposed breaches along the relatively calm Coyote Creek, as well as one breach connecting the Pond to the relatively strong tidal currents of the South Bay. The tidal influences from the breach on the west side of Pond A6 may increase the potential for erosion and further inhibit marsh accumulation from the rates observed in Pond A21.

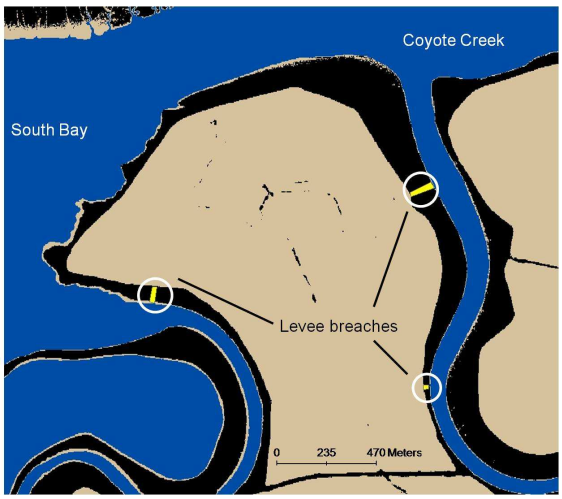

Figure 6. Pond A6 showing the locations of the three proposed levee breaches. The South Bay flows into Coyote Creek near Pond A6.

CONCLUSION

In this study, suspended sediment concentrations were successfully calibrated to remote sensing reflectance values using three statistical techniques: linear regression, multivariate regression, and ANN regression. Multivariate correlations with ASTER provided the best R^2 value of 0.88. The output suspended sediment maps were then used in the MARSED model to predict sediment deposition for Pond A21. Model results show excellent correlation with observed sedimentation rates from Pond A21 with a RMSD of 66.8 mm. This is less than 3 inches of deviation from the observed values. Overall, the model is an accurate predictor of sedimentation for the salt ponds, and can be a useful and successful tool for future management decisions. These tools can aid restoration managers in deciding not only the ideal spots to place a breach, but can also provide an idea of the time frame for the pond to reach equilibrium levels.

ACKNOWLEDGEMENTS

We thank Randy Berthold, John Preston, and Matt Linton for making the NASA DART boats available for our sampling campaign. We also thank Mike Torresan and Angela Lam for providing the USGS facilities for our sediment analysis. We also thank Erin Justice, Dr. Charles Williams, Brad Lobitz, and Dr. David Freyberg for their help and support with this project.

REFERENCES

Allen, J., 1990. Salt-marsh growth and stratification: a numerical model with special reference to the Severn Estuary, southwest Britain, *Marine Geology*, 95: 77–96.

Allen, J., 1997. Simulation models of salt-marsh morphodynamics: some implications for high-intertidal sediment couplets related to sea-level change, *Sedimentary Geology*, 113: 211–223.

Baban, S. M. J., 1995. The use of Landsat imagery to map fluvial sediment discharge into coastal waters, *Marine Geology*, 123 (3–4): 263–270.

Bale, A., 1998. Sediment trap performance in tidal waters: comparison of cylindrical and conical collectors, *Continental Shelf Research*, 18(11): 1401–1418.

Boumans, R., and J. Day, 1993. High precision measurements of sediment elevation in shallow coastal areas using a sedimentation-erosion table, *Estuaries and Coasts*, 16(2): 375–380.

Buchanan, P., and M. A. Lionberger, 2007. Summary of suspended-sediment concentration data, San Francisco Bay, California, water year 2005, U.S. Geological Survey Data Series 282, Reston, VA, 49 pp.

Callaway, J. C., V. T. Parker, L. M. Schile, E. R. Herbert, and E. L. Borgnis, 2009. Dynamics of sediment accumulation in Pond A21 at the Island Ponds, California State Coastal Conservancy, Oakland, CA, 66 pp.

Cahoon, D. R., and J. C. Lynch, 1997. Vertical accretion and shallow subsidence in a mangrove forest of southwestern Florida, USA, *Mangroves and Salt Marshes*, 1(3): 173–186.

Cahoon, D., J. Lynch, P. Hensel, R. Boumans, B. Perez, B. Segura, and J. Day Jr., 2002. High-precision measurements of wetland sediment elevation: I. Recent improvements to the sedimentation-erosion table, *Journal of Sedimentary Research*, 72(5): 730–733.

Chen, Z., P. J. Curran, and J. D. Hansom, 1992. Derivative reflectance spectroscopy to estimate suspended sediment concentration, *Remote Sensing of Environment*, 40(1): 67–77.

Chen, Z., C. Hu, and F. Muller-Karger, 2006. Monitoring turbidity in Tampa Bay using MODIS/Aqua 250-m imagery, *Remote Sensing of Environment*, 109(2): 207–220.

Childers, D., F. Sklar, B. Drake, and T. Jordan, 1993. Seasonal measurements of sediment elevation in three mid-Atlantic estuaries, *Journal of Coastal Research*, 9(4): 986–1003.

Foxgrover, A., B. Jaffe, G. Hovis, C. Martin, J. Hubbard, M. Samant, and S. Sullivan, 2007. 2005 Hydrographic survey of South San Francisco Bay, California, Open-File Report, U.S. Geological Survey, 113 pp.

French, J. R., and T. Spencer, 1993. Dynamics of sedimentation in a tide-dominated back-barrier salt marsh, Norfolk, UK, *Marine Geology*, 110(3–4): 315–331.

French, J. R., T. Spencer, A. L. Murray, and N. S. Arnold, 1995. Geostatistical analysis of sediment deposition in two small tidal wetlands, Norfolk, U.K., *Journal of Coastal Research*, 11(2): 308–321.

Froidefond, J. M., P. Castaing, J. M. Jouanneau, R. Prud'Homme, and A. Dinet, 1993. Method for the quantification of suspended sediments from AVHRR NOAA-11 satellite data, *International Journal of Remote Sensing*, 14(5): 885–894.

Gardner, J., W. Dean, and T. Vallier, 1980. Sedimentology and geochemistry of surface sediments, outer continental shelf, southern Bering Sea, *Marine Geology*, 35(4): 299–329.

Haidvogel, D., H. Arango, W.P. Budgell, B.D. Cornuelle, E. Curchister, E. Di Lorenzo, K.. Fennel, W.R. Geyer, A.J. Hermann, L. Lanerolle, L. Levin, J.C. McWilliams, A.J. Miller, A.M. Moore, T.M. Powell, A.F. Shchepetkin, C.R. Sherwood, R.P. Signell, J.C. Warner, and J. Wilkin, 2008. Ocean forecasting in terrain-following coordinates: Formulation and skill assessment of the Regional Ocean Modeling System, *Journal of Computational Physics*, 227(7): 3595–3624.

Krone, R., 1987. A method for simulating historic marsh elevations, in Kraus, N. (Ed.), *Coastal Sediments 87*, American Society of Civil Engineers, New York, New York, pp. 316–323.

Li, R., Y. Kaufman, Bo-Cai Gao, and C. Davis, 2003. Remote sensing of suspended sediments and shallow coastal waters, *IEEE Transactions on Geology and Remote Sensing*, 41(3): 559–566.

Miller, R. L., and B. A. McKee, 2004. Using MODIS Terra 250 m imagery to map concentrations of total suspended matter in coastal waters, *Remote Sensing of Environment*, 93(1–2): 259–266.

Munday Jr., J. C., and T. T. Alföldi, 1979. LANDSAT test of diffuse reflectance models for aquatic suspended solids measurement, *Remote Sensing of Environment*, 8(2): 169–183.

NCDC, National Climate Data Center, 2010. National Environmental Satellite, Data, and Information Service, National Oceanic and Atmospheric Administration, http://www.ncdc.noaa.gov/oa/ncdc.html. (Accessed 10 July, 2010).

Pasternack, G. B., and G. S. Brush, 1998. Sedimentation cycles in a river-mouth tidal freshwater marsh, *Estuaries and Coasts*, 21(3): 407–415.

Philip Williams & Associates, Ltd., 2005. Hydrodynamics and sediment dynamics: existing conditions report, South Bay Salt Pond Restoration Project, California State Coastal Conservancy, U.S. Fish & Wildlife Service, California Department of Fish and Game, 88 pp.

Philip Williams & Associates, Ltd, P. M., and P. M. Faber, 2004. Design guidelines for tidal wetland restoration in San Francisco Bay, The Bay Institute and California State Coastal Conservancy, Oakland, CA, 83 pp.

Reed, D. J., 1989. Patterns of sediment deposition in subsiding coastal salt marshes, Terrebonne Bay, Louisiana: the role of winter storms, *Estuaries and Coasts*, 12(4): 222–227.

Ruhl, C. A., D. H. Schoellhamer, R. P. Stumpf, and C. L. Lindsay, 2001. Combined use of remote sensing and continuous monitoring to analyze the variability of suspended-sediment concentrations in San Francisco Bay, California, *Estuarine, Coastal and Shelf Science*, *53*(6): 801–812

SI Metric, 2010. Mass, Weight, Density, or Specific Gravity of Bulk Materials, SI Metric. [online] Available from: http://www.simetric.co.uk/si_materials.htm. (Accessed 9 August, 2010).

Stumpf, R. P., and J. R. Pennock, 1989. Calibration of a general optical equation for remote sensing of suspended sediments on a moderately turbid estuary, *Journal of Geophyical Research*, *94*(C10): 363–377.

Takekawa, J. Y., A. K. Miles, D. H. Schoellhamer, B. Jaffe, N. D. Athearn, S. E. Spring, G. G. Shellenbarger, M. K. Saiki, F. Mejia, and M. A. Lionberger, 2005. South Bay Salt Ponds Restoration Project, Short-term Data Needs, 2003–2005, Unpubl. Final Report, U.S. Geological Survey, Vallejo, CA, 270 pp.

Temmerman, S., G. Govers, P. Meire, and S. Wartel, 2003. Modelling long-term tidal marsh growth under changing tidal conditions and suspended sediment concentrations, Scheldt estuary, Belgium, *Marine Geology*, 193(1–2): 151–169.

Temmerman, S., G. Govers, S. Wartel, and P. Meire, 2004. Modelling estuarine variations in tidal marsh sedimentation: response to changing sea level and suspended sediment concentrations, *Marine Geology*, 212(1–4): 1–19.

Teodoro, A., F. Veloso-Gomes, and H. Gonçalves, 2008. Statistical techniques for correlating total suspended matter concentration with seawater reflectance using multispectral satellite data, *Journal of Coastal Research*, *24*(3): 40.

Trulio, L., D. Clarke, S. Ritchie, and A. Hutzel, 2007. South Bay salt pond restoration project: adaptive management plan, Final Environmental Impact Statement Report, South Bay Salt Pond Restoration Project, CA, 143 pp.

USGS, 2007. Continuous monitoring in the San Francisco Bay and Delta, U.S. Geological Survey. [online] Available from: http://sfbay.wr.usgs.gov/sediment/Cont_monitoring/index.html. (Accessed 14 June, 2010).

USGS, 2010a. Global Visualization Viewer, Earth Resources Observation and Science Center, (Glovis) http://glovis.usgs.gov/. (Accessed 10 July, 2010).

USGS, 2010b. Water quality monitoring of San Francisco Bay, U.S. Geological Survey. [online] Available from: http://sfbay.wr.usgs.gov/access/wqdata. (Accessed 14 June, 2010).

Wilde, I., F. Neural Networks, Mathematics Department, King's College London. [online] Available from: http://homepage.ntlworld.com/ivan.wilde/notes/nn/nnnotespdf.pdf. (Accessed 19 August, 2010).

WIST, Warehouse Inventory Search Tool, 2010. Land Process Distributed Active Archive Center, National Aeronautics and Space Administration, https://lpdaac.usgs.gov/lpdaac/get_data/wist. (Accessed 22 July, 2010).